Composite Structures 157 (2016) 275–284

Contents lists available at ScienceDirect

Composite Structures

journal homepage: www.elsevier.com/locate/compstruct

Viscoelastic properties of heterogeneous materials: The case of periodic media containing cuboidal inclusions

Sy-Tuan Nguyen [a,b,*], Quy-Dong To [b,c], Minh-Ngoc Vu [b], Thê-Duong Nguyen [b]

[a] Euro-Engineering, rue Jules Ferry, 64053 Pau, France
[b] Duy Tan University, Institute of Research & Development, K7/25 Quang Trung, Danang, Viet Nam
[c] Universite Paris-Est, Laboratoire Modelisation et Simulation Multi Echelle, MSME UMR 8208 CNRS, 5 Boulevard Descartes, 77454 Marne-la-Vallee Cedex 2, France

ARTICLE INFO

Article history:
Received 4 June 2016
Revised 31 July 2016
Accepted 1 September 2016
Available online 4 September 2016

Keywords:
Viscoelastic
Homogenization
Laplace-Carson transform
Cuboidal inclusions

ABSTRACT

This paper presents analytical solutions for the effective viscoelastic properties of composite materials based on a homogenization approach. The cases of spherical inclusions and cracks were recently developed. The objective of this paper is to use the same technique to deal with the case of periodic media containing cuboidal inhomogeneities. The viscoelastic behavior of both the matrix and the homogeneous equivalent medium is modeled by the Zener rheological model while inclusions are assumed to be linearly elastic. The viscoelastic Hill tensor required for the calculation of the effective viscoelastic tensors is obtained explicitly in the Laplace-Carson space in terms of Fourier series. The final expressions show that overall behavior depends on the viscoelastic properties of the matrix, the 3D dimensions of the inclusions and the thickness of the matrix layer between two nearby inclusions. Applications to masonry structures are presented to illustrate the theoretical results.

1. Introduction

Viscoelastic behavior exhibits in many natural and artificial materials such as concrete, masonry, rock, etc and effective viscoelastic properties are needed to model structures made of those materials. In laboratories, the elastic moduli and viscosity of materials can be obtained from creep and relaxation tests. However, such experiments usually take months or years [8]. Moreover, for heterogeneous and anisotropic materials, numerous tests are required to capture all the possibilities of the variation of the microstructure and the volume fractions of the constituents. These difficulties can be overcome by using the numerical codes (finite element method, boundary element method, etc). However, a considerable amount of computation cost is required to study the overall behavior of anisotropic heterogeneous viscoelastic materials due to the complexity of the microstructure and the non linear stress-strain relationship.

For many decades, the micromechanical approach is proved to be a powerful tool to determine the effective elastic or viscoelastic properties of anisotropic heterogeneous materials [6,7,3,24,27,9,12,5]. For elastic materials, many analytical solutions are available for the estimation of their effective elastic moduli from the microstructure information. For the case of viscoelastic materials, the Laplace-Carson (LC) transform technique is usually considered. The correspondence principle allows considering a linear viscoelastic material as an equivalent elastic one in LC space. The analytical solutions obtained for elastic materials can be employed to calculate the overall effective viscoelastic stiffness tensor in LC space and the inverse LC transform is usually used to transform these solutions to time space [14,13]. This technique remains complex and sometime impossible due to the complexity of the inverse LC transform.

To overcome this difficulty, Nguyen and colleagues [17,18] proposed a technique that does not require the complex inverse LC transformation. The idea is to determine the effective rheological viscoelastic properties directly in LC space by considering the short and long terms behaviors with adequate verification in transient condition. This technique was successfully used for cracked material [19,20,21], cracked heterogeneous material containing spherical inclusions [23] and porous media [22].

The objective of this paper is to apply such technique to study periodic media containing elastic cuboidal inclusions, for example of the case of masonry structures. The Standard Linear Solids (SLS) model (Zener rheological model) (Fig. 1) is used for the matrix and the equivalent homogeneous medium, and the linear elastic model for the inclusions. The viscoelastic periodic Hill tensor, required for the calculation of the effective viscoelastic tensors, is firstly

* Corresponding author at: Euro-Engineering, rue Jules Ferry, 64053 Pau, France.
E-mail addresses: stuan.nguyen@gmail.com (S.-T. Nguyen), quy-dong.to@u-pem.fr (Q.-D. To), vungocminh@dtu.edu.vn (M.-N. Vu), theduong.nguyen@duytan.edu.vn (T.-D. Nguyen).

http://dx.doi.org/10.1016/j.compstruct.2016.09.003
0263-8223/

Notations

$\sigma, \boldsymbol{\Sigma}$	microscopic and macroscopic stress tensors
$\boldsymbol{\varepsilon}, \boldsymbol{E}$	microscopic and macroscopic strain tensors
$\mathbb{c}, \mathbb{C}$	microscopic and macroscopic viscoelastic stiffness tensors
$\mathbb{A}, \mathbb{P}$	localization and Hill's tensors
$\mathbb{W}, \mathbb{U}$	geometric tensors
$\mathbf{1}, \mathbb{I}$	second and fourth order identity tensors
k, μ, λ	bulk and Lamé's viscoelastic properties
f	volume fraction of inclusions
b_1, b_2, b_3	3D dimensions of inclusions
a_1, a_2, a_3	3D dimensions of a unit periodic cell
S_1 to S_9	components of the geometric tensors
ξ_1 to ξ_3	components of the wave vector
p	Laplace-Carson variable
p^{α}_{β}	components of the Hill's tensor
$*$	superscript stands for Laplace-Carson transform values
hom	index or superscript stand for homogenous values
M	index stands for Maxwell's series
∞, ins	indexes stand for long-term and instantaneous properties
$0, i$	indexes stand for matrix and inclusions
v	index or superscript stands for viscosity
$\mathcal{O}(.)$	negligible value

obtained explicitly in LC space and in the form of a Fourier series. Next, we derive analytical expressions for the effective properties from the parameters of the constituents, i.e. mechanical properties, geometries and spatial arrangements. Finally, theoretical development is validated and applied to study the viscoelastic behavior of masonry with sensitivity analysis.

2. Homogenization theory of viscoelastic heterogeneous media

In LC space, the overall viscoelastic properties of heterogeneous media can be obtained by establishing the relationship between the local behavior

$$\boldsymbol{\sigma}^*(\boldsymbol{x}) = \mathbb{c}^*(\boldsymbol{x}) : \boldsymbol{\varepsilon}^*(\boldsymbol{x}) \tag{1}$$

and the macroscopic behavior of a representative elementary volume (REV):

$$\boldsymbol{\Sigma}^* = \mathbb{C}^*_{hom} : \mathbf{E}^* \tag{2}$$

$$\boldsymbol{\Sigma}^* = \frac{1}{|V|}\int_V \boldsymbol{\sigma}^*(\boldsymbol{x})dV \tag{3}$$

$$\mathbf{E}^* = \frac{1}{|V|}\int_V \boldsymbol{\varepsilon}^*(\boldsymbol{x})dV \tag{4}$$

In Eqs. (1)–(4) and the remaining part of the paper, the superscript "$*$" stands for the LC transform of the corresponding quantities, for example:

$$\varphi^*(\boldsymbol{x}, p) = p\int_0^\infty \varphi(\boldsymbol{x}, t)e^{-pt}dt \tag{5}$$

In this case, $\boldsymbol{\sigma}^*(\boldsymbol{x})$, $\boldsymbol{\varepsilon}^*(\boldsymbol{x})$ and $\mathbb{c}^*(\boldsymbol{x})$ are the local stress, strain and stiffness tensors at a point $\boldsymbol{x}$ inside the REV in LC space. The quantities $\boldsymbol{\Sigma}^*$, $\mathbf{E}^*$ and $\mathbb{C}^*_{hom}$ are respectively the average stress and strain tensors and the effective stiffness tensor of the REV. The notation V stands for the volume of the REV. The local and the average strain tensors are related by the following linear equation:

$$\boldsymbol{\varepsilon}^*(\boldsymbol{x}) = \mathbb{A}^*(\boldsymbol{x}) : \mathbf{E}^* \tag{6}$$

where $\mathbb{A}^*(\boldsymbol{x})$ is the strain localization tensor at a point $\boldsymbol{x}$. The combination of equations from (1) to (6) yields the following equation to calculate the overall stiffness tensor of the REV:

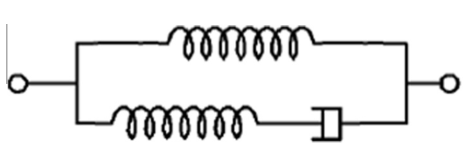

Fig. 1. The Standard Linear Solid model used for the matrix and the effective material.

$$\mathbb{C}^*_{hom} = \frac{1}{V}\int_V \mathbb{C}^*(\boldsymbol{x}) : \mathbb{A}^*(\boldsymbol{x})dV \tag{7}$$

The derivation of $\mathbb{C}^*_{hom}$ from (6) and (7) summarizes the strain based procedure, equivalent to the dual stress based procedure [4]. In Eq. (7), the local stiffness tensor $\mathbb{C}^*(\boldsymbol{x})$ is assumed to be known and the main question is to determine the strain localization tensor $\mathbb{A}^*(\boldsymbol{x})$. The later must verify the following condition:

$$\frac{1}{V}\int_V \mathbb{A}^*(\boldsymbol{x})dV = \mathbb{I} \tag{8}$$

Taking the matrix as the reference material (the host material) with property $\mathbb{C}^*_0$ and considering n inclusions as inhomogeneities with properties $\mathbb{C}^*_i$ (i = 1,2 ..., n), from Eqs. (7) and (8), we can write the effective tensor as:

$$\mathbb{C}^*_{hom} = \mathbb{C}^*_0 + \sum_{i=1}^{n} f_i(\mathbb{C}^*_i - \mathbb{C}^*_0) : \mathbb{A}^*_i \tag{9}$$

The remaining parameters f_i and $\mathbb{A}^*_i$ are respectively the volume fraction and the average localization tensor of the inhomogeneity *i*.

In what follows, we shall consider the case of two phases composite made of one specy of inhomogeneity (n = 1). The inhomogeneities (or inclusions) are elastic, or $\mathbb{C}^*_1 = \mathbb{C}_1$ and only the matrix material is viscoelastic. The behavior of the latter is modeled by a rheological model composed of three elements (two springs and one dash-pot) as shown in Fig. 1. It is a Maxwell series in parallel with the second spring that defines the long term elastic behavior of the material. In LC space, the elastic stiffness of the equivalent elastic material is a function of the LC variable p and the properties of the rheological elements (see also [18]. In this case, this dependency is expressed as:

$$\mathbb{C}^*_0 = \left(\mathbb{C}_M^{-1} + \frac{1}{p}\mathbb{C}_v^{-1}\right)^{-1} + \mathbb{C}_\infty \tag{10}$$

where $\mathbb{C}_M$ is the elastic stiffness tensor corresponding to the spring of the Maxwell series, $\mathbb{C}_v$ the viscosity tensor of the dash-pot and $\mathbb{C}_\infty$ the elastic stiffness tensor of the second spring that corresponds also to the long-term elastic behavior of the material.

3. Two phases viscoelastic periodic composite

3.1. Integral formulation of eigenstrain and approximation

We consider a special microstructure where the inclusions are arranged periodically in space with periods a_1, a_2, a_3 along the three directions 1, 2 and 3. In the case of elastic materials, Nemat-Nasser et al. [15] proposed an estimation scheme based on integral equation approach. Due to the correspondence principle, the same method can be applied to the viscoelastic materials. Indeed, introducing first the periodic eigenstrain $\tilde{\varepsilon}^*$ field as

$$\mathbb{C}_0^* : (\boldsymbol{\varepsilon}^* - \tilde{\boldsymbol{\varepsilon}}^*) = \boldsymbol{\sigma}^* \tag{11}$$

the following relation can be obtained

$$\boldsymbol{\varepsilon}^* = \boldsymbol{E}^* + \Gamma^{0*}(\mathbb{C}_0^* : \tilde{\varepsilon}^*) \tag{12}$$

In Eq. (12), the operator Γ^{0*} admits the analytical form in the Fourier space:

$$\Gamma^{0*}_{ijkl}(\xi) = \frac{1}{4\mu_0^*}\frac{\delta_{ik}\xi_j\xi_l + \delta_{il}\xi_j\xi_k + \delta_{jk}\xi_i\xi_l + \delta_{jl}\xi_i\xi_k}{\xi_1^2+\xi_2^2+\xi_3^2} - \frac{\lambda_0^*+\mu_0^*}{\mu_0^*(\lambda_0^*+2\mu_0^*)}\frac{\xi_i\xi_j\xi_k\xi_l}{(\xi_1^2+\xi_2^2+\xi_3^2)^2} \tag{13}$$

with ξ_i $(i = 1, 2, 3)$ being the components of the wave vector ξ:

$$\xi_i = \frac{2\pi n_i}{a_i}, \; n_i \in \mathbb{Z} \tag{14}$$

With the help of the Fourier transform, we can write the convolution product between Γ^{0*} and a periodic second order tensor $\boldsymbol{a}(\boldsymbol{x})$ as

$$\Gamma^{0*}\boldsymbol{a} = \sum_{\xi\neq\boldsymbol{0}}\Gamma^{0*}(\xi) : \boldsymbol{a}(\xi)e^{i\xi.x} \tag{15}$$

where $\boldsymbol{a}(\xi)$ is the Fourier transform of $\boldsymbol{a}(\boldsymbol{x})$

$$\boldsymbol{a}(\xi) = \frac{1}{V}\int_V \boldsymbol{a}(\boldsymbol{x})e^{-i\xi.x}d\boldsymbol{x} \tag{16}$$

and V being the unit cell $V = a_1 \times a_2 \times a_3$.

Using the relation between stress and strain, Eq. (12) can be recast in the form of an integral equation

$$\mathbb{C}_0^* : \tilde{\boldsymbol{\varepsilon}}^* = (\mathbb{C}_0^* - \mathbb{C}_1) : (\boldsymbol{E} + \Gamma^{0*}(\mathbb{C}_0^* : \tilde{\boldsymbol{\varepsilon}}^*)) \tag{17}$$

Next, we average both sides of (17) over the inclusion volume Ω, notation $\langle . \rangle_\Omega$, and estimate $\langle\tilde{\boldsymbol{\varepsilon}}^*\rangle_\Omega$. Making approximation that $\tilde{\boldsymbol{\varepsilon}}^*$ equal to its average $\langle\tilde{\boldsymbol{\varepsilon}}^*\rangle_\Omega$ when evaluating the integral related to Γ^{0*}, we find that

$$\langle\Gamma^{0*}(\mathbb{C}_0^* : \tilde{\boldsymbol{\varepsilon}}^*)\rangle_\Omega \approx \langle\Gamma^{0*}\chi\rangle_\Omega : \mathbb{C}_0^* : \langle\tilde{\boldsymbol{\varepsilon}}^*\rangle_\Omega = \mathbb{S}^* : \langle\tilde{\boldsymbol{\varepsilon}}^*\rangle_\Omega \tag{18}$$

Here the characteristic function $\chi(\xi)$ is defined as being equal to 1 for points inside inclusion and vanished outside. To et al. [26] showed that $\mathbb{S}^* = \langle\Gamma^{0*}\chi\rangle_\Omega : \mathbb{C}_0^*$ is the periodic Eshelby tensor. Different from the classical Eshelby problem involving one isolated inclusion, the inclusions here are distributed periodically in space and can interact. As a result, the final tensor $\mathbb{S}^*$ here can be viewed as superposition of the interior solution and many exterior solutions due to the eigenstrain of the surrounding ones. This tensor does not only depend on the shape of the inclusions but also on the periods a_1, a_2, a_3, or the cell's dimensions.

Returning to our problem, we find that the tensor $\mathbb{P}^* = \langle\Gamma^{0*}\chi\rangle_\Omega$ plays a similar role as the classical Hill tensor whose Fourier series expression can be written explicitly as

$$\mathbb{P}^* = \sum_{\xi\neq 0} f^{-1}\chi(\xi)\chi(-\xi)\Gamma^{0*}(\xi) = \sum_{\xi\neq 0} p(\xi)\Gamma^{0*}(\xi) \tag{19}$$

The geometric function $p(\xi) = f^{-1}\chi(\xi)\chi(-\xi)$ appeared in (19) depends only on the form factor $\chi(\xi)$ (the Fourier transform of the characteristic function) and the volume fraction f of the inclusions. From (17), one can obtain immediately $\langle\tilde{\boldsymbol{\varepsilon}}^*\rangle_\Omega$ in terms of $\boldsymbol{E}^*$ and then the localization tensor in this phase

$$\mathbb{A}_1^* = [\mathbb{I} + \mathbb{P}^* : (\mathbb{C}_1 - \mathbb{C}_0^*)]^{-1} \tag{20}$$

Finally, substituting (20) into (9) yields the expression of the effective stiffness of the considering composite

$$\mathbb{C}^*_{hom} = \mathbb{C}_0^* + f[(\mathbb{C}_1 - \mathbb{C}_0^*)^{-1} + \mathbb{P}^*]^{-1} \tag{21}$$

From the first appearance, it seems that the expression (21) resulted from the present approximation corresponds to the dilute scheme. However, we must recall here that the tensor $\mathbb{P}^*$ associated to the periodic structure have already accounted for the interaction between the inclusions.

3.2. General analysis of the overall behavior

Generally, obtaining explicit expression of $\mathbb{C}^*_{hom}$ in LC space is always possible. However, it is much more difficult to find the corresponding results in time space by LC inverse transform. To overcome this difficulty, we approximate the overall behavior by the SLS model and derive the rheological parameters by studying the long term and short term behaviors of the equivalent materials. Without assuming any particular inclusion shapes, we shall analyze first all the quantities involved in (21) and their impacts on $\mathbb{C}^*_{hom}$. The series expansion of $\mathbb{C}_0^*$ in the vicinity of $p = 0$ reads:

$$\mathbb{C}_0^* = \mathbb{C}_\infty + p\mathbb{C}_v + \mathcal{O}(p^2) \tag{22}$$

Analogously, the Hill tensor can be approximated by:

$$\mathbb{P}^* = \mathbb{P}_\infty + p\mathbb{P}_v + \mathcal{O}(p^2) \tag{23}$$

where $\mathbb{P}_\infty$ corresponds to the long term Hill tensor. The combination of Eqs. (22), (23) and (20) also leads to the following formula for the localization tensor when $p \to 0$:

$$\mathbb{A}^* = \mathbb{A}_\infty + p\mathbb{A}_v + \mathcal{O}(p^2) \tag{24}$$

where

$$\mathbb{A}_\infty = (\mathbb{I} + \mathbb{P}_\infty : (\mathbb{C}_1 - \mathbb{C}_\infty))^{-1} \tag{25}$$

and

$$\mathbb{A}_v = -(\mathbb{P}_v : (\mathbb{C}_1 - \mathbb{C}_\infty) - \mathbb{P}_\infty : \mathbb{C}_v) : (\mathbb{A}_\infty : \mathbb{A}_\infty) \tag{26}$$

Based on Eqs. (22), (24) and (21), the overall tensor $\mathbb{C}^*_{hom}$ can be written as:

$$\mathbb{C}^*_{hom} = \mathbb{C}_{\infty hom} + p\mathbb{C}_{v hom} + \mathcal{O}(p^2) \tag{27}$$

where

$$\mathbb{C}_{\infty hom} = \mathbb{C}_\infty + f(\mathbb{C}_1 - \mathbb{C}_\infty) : \mathbb{A}_\infty \tag{28}$$

and

$$\mathbb{C}_{v hom} = \mathbb{C}_v + f((\mathbb{C}_1 - \mathbb{C}_\infty) : \mathbb{A}_v - \mathbb{C}_v : \mathbb{A}_\infty) \tag{29}$$

Regarding the short term behavior ($p \to \infty$), the tensor $\mathbb{C}_0^*$ can be approximated by the expression

$$\mathbb{C}_0^* = \mathbb{C}_{ins} + \mathcal{O}\left(\frac{1}{p}\right) \tag{30}$$

with the instantaneous stiffness tensor being defined by:

$$\mathbb{C}_{ins} = \mathbb{C}_M + \mathbb{C}_\infty \tag{31}$$

Next, the asymptotic response at $p \to \infty$ of the Hill tensor $\mathbb{P}^*$ can be calculated with the formula

$$\mathbb{P}^* = \mathbb{P}_{ins} + \mathcal{O}\left(\frac{1}{p}\right) \tag{32}$$

where $\mathbb{P}_{ins}$ is the instantaneous Hill tensor. Finally, using the approximation (30) and (32), the localization tensor $\mathbb{A}^*$ and then the homogenized stiffness tensor $\mathbb{C}^*_{hom}$ can be approximated by:

$$\mathbb{A}^* = \mathbb{A}_{ins} + \mathcal{O}\left(\frac{1}{p}\right) \tag{33}$$

$$\mathbb{C}^*_{hom} = \mathbb{C}^{hom}_{ins} + \mathcal{O}\left(\frac{1}{p}\right) \tag{34}$$

Here, we introduce the instantaneous localization tensor as:

$$\mathbb{A}_{ins} = (\mathbb{I} + \mathbb{P}_{ins} : (\mathbb{C}_1 - \mathbb{C}_{ins}))^{-1} \tag{35}$$

and the instantaneous homogenized stiffness tensor as:

$$\mathbb{C}^{hom}_{ins} = \mathbb{C}_{ins} + f(\mathbb{C}_1 - \mathbb{C}_{ins}) : \mathbb{A}_{ins} \tag{36}$$

Finally, the homogenized stiffness tensor $\mathbb{C}_{Mhom}$ is given by the expression:

$$\mathbb{C}_{Mhom} = \mathbb{C}^{hom}_{ins} - \mathbb{C}_{\infty hom} \tag{37}$$

Eqs. (27) and (34) allow estimating the effective viscoelastic behavior of the mixture by the same SLS rheological model as the matrix

$$\mathbb{C}^*_{hom} = \left(\mathbb{C}^{-1}_{Mhom} + \frac{1}{p}\mathbb{C}^{-1}_{vhom}\right)^{-1} + \mathbb{C}_{\infty hom} \tag{38}$$

where the effective viscoelastic tensors $\mathbb{C}_{Mhom}$, $\mathbb{C}_{vhom}$ and $\mathbb{C}_{\infty hom}$ are determined by Eqs. (37), (29) and (28), respectively. They are functions of the elastic properties and the volume fraction of the inclusions ($\mathbb{C}_1$ and f) as well as the viscoelastic properties of the matrix ($\mathbb{C}_M$, $\mathbb{C}_v$ and $\mathbb{C}_\infty$). The Hill tensors $\mathbb{P}_{ins}$, $\mathbb{P}_v$ and $\mathbb{P}_\infty$ required for the calculations will be derived in Section 3 for the case of periodic composite with cuboidal inclusions.

3.3. Case of cuboidal inclusion

For cuboidal inclusion of dimensions $\Omega = b_1 \times b_2 \times b_3$, the geometric function $p(\xi)$ becomes

$$p(\xi) = f\prod_{i=1}^{3}\left[\frac{\sin\left(\frac{\xi_i b_i}{2}\right)}{\left(\frac{\xi_i b_i}{2}\right)}\right]^2 \tag{39}$$

We can recast the Hill tensor in the following form

$$\mathbb{P}^* = p^*_w\mathbb{W} + p^*_u\mathbb{U} \tag{40}$$

where $\mathbb{W}$ and $\mathbb{U}$ are fourth order geometric tensors. The parameters p^*_w and p^*_u are functions of the viscoelastic properties of the matrix:

$$p^*_w = \frac{1}{2\mu^*_0} \tag{41}$$

and

$$p^*_u = -\frac{\lambda^*_0 + \mu^*_0}{\mu^*_0(\lambda^*_0 + 2\mu^*_0)} \tag{42}$$

The tensors $\mathbb{W}$ and $\mathbb{U}$ are two geometric tensors that are not affected by the LC transform:

$$\mathbb{W} = \begin{bmatrix} 2S_1 & 0 & 0 & 0 & 0 & 0 \\ 0 & 2S_2 & 0 & 0 & 0 & 0 \\ 0 & 0 & 2S_3 & 0 & 0 & 0 \\ 0 & 0 & 0 & S_2+S_3 & 0 & 0 \\ 0 & 0 & 0 & 0 & S_1+S_3 & 0 \\ 0 & 0 & 0 & 0 & 0 & S_1+S_2 \end{bmatrix} \tag{43}$$

and

$$\mathbb{U} = \begin{bmatrix} S_4 & S_9 & S_8 & 0 & 0 & 0 \\ S_9 & S_5 & S_7 & 0 & 0 & 0 \\ S_8 & S_7 & S_6 & 0 & 0 & 0 \\ 0 & 0 & 0 & 2S_7 & 0 & 0 \\ 0 & 0 & 0 & 0 & 2S_8 & 0 \\ 0 & 0 & 0 & 0 & 0 & 2S_9 \end{bmatrix} \tag{44}$$

where the geometric scalars S_1 to S_9 are the lattice sums given by:

$$S_i = \sum_{\xi\neq 0} p(\xi)\frac{\xi_i^2}{\xi_1^2 + \xi_2^2 + \xi_3^2} \tag{45}$$

$$S_{i+3} = \sum_{\xi\neq 0} p(\xi)\frac{\xi_i^4}{\left(\xi_1^2 + \xi_2^2 + \xi_3^2\right)^2} \tag{46}$$

$$S_{i+6} = \sum_{\xi\neq 0} p(\xi)\frac{\xi_j^2\xi_k^2}{\left(\xi_1^2 + \xi_2^2 + \xi_3^2\right)^2} \tag{47}$$

The viscoelastic tensors of the matrix can be decomposed into spherical and deviatoric parts as:

$$\mathbb{C}_M = 3k_M\mathbb{J} + 2\mu_M\mathbb{K} \tag{48}$$

$$\mathbb{C}_v = 3k^v_M\mathbb{J} + 2\mu^v_M\mathbb{K} \tag{49}$$

$$\mathbb{C}_\infty = 3k_\infty\mathbb{J} + 2\mu_\infty\mathbb{K} \tag{50}$$

where the springs are characterized by the bulk and the shear elastic moduli denoted by k_M and μ_M for Maxwell one and k_∞ and μ_∞ for the second one. On the other hand, the dash-pot of the Maxwell series is represented by the bulk and shear viscosities k^v_M and μ^v_M. The fourth order tensors $\mathbb{J} = \mathbf{1}\otimes\mathbf{1}/3$ and $\mathbb{K} = \mathbb{I} - \mathbb{J}$ are the spherical and deviatoric parts of the unit tensor respectively, with 1 is the second order unit tensor and $\mathbb{I}$ the fourth order unit tensor. Employing the asymptotic behavior analysis in the previous section, Eq. (22) leads to the following approximation of the Lamé's moduli:

$$\mu^*_0 = \mu_\infty + p\mu^v_M + \mathcal{O}(p^2) \tag{51}$$

$$\lambda^*_0 = \lambda_\infty + p\lambda^v_M + \mathcal{O}(p^2) \tag{52}$$

where $\lambda_\infty = k_\infty - \frac{2}{3}\mu_\infty$ and $\lambda^v_M = k^v_M - \frac{2}{3}\mu^v_M$. The introduction of Eqs. (51) and (52) in Eqs. (41) and (42) results the following approximation of the Hill's parameters p^*_w and p^*_u when $p \to 0$:

$$p^*_w = p^\infty_w + pp^v_w + \mathcal{O}(p^2) \tag{53}$$

$$p^*_u = p^\infty_u + pp^v_u + \mathcal{O}(p^2) \tag{54}$$

with

$$p^\infty_w = \frac{1}{2\mu_\infty};\; p^v_w = -\frac{\mu^v_M}{2\mu^2_\infty} \tag{55}$$

and

$$p^\infty_u = -\frac{\lambda_\infty + \mu_\infty}{\mu_\infty(\lambda_\infty + 2\mu_\infty)};\; p^v_u = \left(\frac{\lambda^v_M + \mu^v_M}{\lambda_\infty + \mu_\infty} - \frac{\mu^v_M}{\mu_\infty} - \frac{\lambda^v_M + 2\mu^v_M}{\lambda_\infty + 2\mu_\infty}\right)p^\infty_u \tag{56}$$

Besides, when $p \to \infty$, we must obtain the short term response as follows:

$$p^*_w = p^{ins}_w + \mathcal{O}\left(\frac{1}{p}\right);\; p^*_u = p^{ins}_u + \mathcal{O}\left(\frac{1}{p}\right) \tag{57}$$

with

$$p_w^{ins} = \frac{1}{2\mu_{ins}};\ p_u^{ins} = -\frac{\lambda_{ins} + \mu_{ins}}{\mu_{ins}(\lambda_{ins} + 2\mu_{ins})} \quad (58)$$

where

$$\mu_{ins} = \mu_M + \mu_\infty; \lambda_{ins} = \lambda_M + \lambda_\infty \quad (59)$$

Based on the set of Eqs. (51), (52), (57) and (58), we find the relations:

$$\mathbb{P}_{ins} = p_w^{ins}\mathbb{W} + p_u^{ins}\mathbb{U} \quad (60)$$

$$\mathbb{P}_v = p_w^v\mathbb{W} + p_u^v\mathbb{U} \quad (61)$$

$$\mathbb{P}_\infty = p_w^\infty\mathbb{W} + p_u^\infty\mathbb{U} \quad (62)$$

The introduction of Eqs. (60)–(62) in Eqs. (25), (26) and (35) allows calculating the localization tensors that can be then used in Eqs. (28), (29), (36) and (37) to obtain the effective viscoelastic properties of the mixture.

One the effective viscoelastic tensor of the mixture is calculated, the effective stress and strain tensors can be related by following equations (see also Fig. 1):

$$\boldsymbol{\Sigma} = \boldsymbol{\Sigma}_1 + \boldsymbol{\Sigma}_2 \quad (63)$$

$$\boldsymbol{\Sigma}_2 = \mathbb{C}_{\infty hom} : \boldsymbol{E} \quad (64)$$

$$\mathbb{S}_{Mhom} : \dot{\boldsymbol{\Sigma}}_1 + \mathbb{S}_{vhom} : \boldsymbol{\Sigma}_1 = \dot{\boldsymbol{E}} \quad (65)$$

The combination of Eqs. (63)–(65) yields the differential equation

$$\mathbb{S}_{vhom} : \boldsymbol{\Sigma} + \mathbb{S}_{Mhom} : \dot{\boldsymbol{\Sigma}} = \mathbb{S}_{vhom} : \mathbb{C}_{\infty hom} : \boldsymbol{E} + [\mathbb{I} + \mathbb{S}_{Mhom} : \mathbb{C}_{\infty hom}] : \dot{\boldsymbol{E}} \quad (66)$$

that can be used to solve the effective stress and strain fields.

3.4. Validation of the solution in LC space by finite element method

As effective stiffness tensors in LC space given by Eqs. (21) and (40)–(47) are derived with assumption of homogeneous eigenstrain in inclusions, it is important to validate such assumption. To this end, we consider the equivalent elastic problem of a composite containing a homogeneous elastic matrix and cuboidal elastic inclusions. The exact results of the effective elastic properties of such material can be obtained by finite element method (FEM) [16,10,11,25]. For this particular case of periodic medium, to minimize the computational time, finite element calculations can be realized on a unit cell embedding a single cuboidal inclusion with appropriate prescribed periodic boundary conditions [1,2]. It is worth noting that the convergence of the numerical simulation with respect to the element size must be carefully checked to capture the exact response of the composite material. One the numerical results are converged, it can be used as reference to validate the analytical approach. Fig. 2 show a good coherent between the analytical solution and the results obtained by FEM for the shear moduli in three directions.

4. Numerical results and sensitivity analysis

4.1. An application of masonry

To illustrate the analytical solutions derived in previous sections for effective viscoelastic properties of periodic media containing cuboidal inclusions, we consider a stack-bond masonry wall made of viscoelastic mortar matrix and elastic cuboidal brick inclusions. The materials properties of the materials are given in Table 1. The dimensions of the inclusions are $200 \times 50 \times 100$ (mm^3). Fig. 3–5 show the effective viscoelastic properties of the mixture as functions of the volume fraction of bricks. There are three effective viscoelastic stiffness tensors due to the chosen Zener's viscoelastic rheological model for the behavior of the material. Each tensor has nine independent viscoelastic parameters due to the orthotropic anisotropy of the mixture that is result of the cuboidal shape of brick. Figs. 3 and 4 show the long-term effective elastic stiffnesses and that of the Maxwell's series, respectively. Fig. 5 presents the effective viscosities of the Maxwell's series. The terms C_{kkkk} with $k = 1$ to 3 coincide when the volume fraction of inclusions tends to 0 or 1 due to the isotropy of the matrix and inclusions. However they are very different at about 60–80% inclusion volume fraction. Similar trends are obtained for the terms C_{ijij} and C_{iijj}. It is interesting to observe that all the elastic stiffnesses and the viscosities of the Maxwell's series tend to zero when the volume fraction of brick tends to 1. It is evident since the elastic behavior assumed for brick

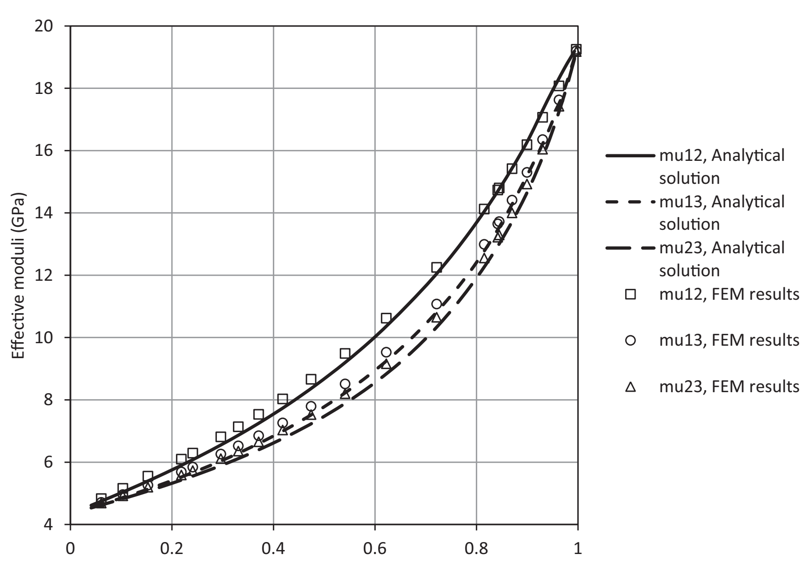

Fig. 2. Effective shear modulus in LC space: comparison of the developed model and the numerical simulation using FEM.

Table 1
Viscoelastic properties of matrix and inclusion used for the simulations [23].

Parameters	Values	Units
k_M	2.404	GPa
μ_M	1.655	GPa
k_M^v	23.639	GPa·h
μ_M^v	21.375	GPa·h
k_∞	1.257	GPa
μ_∞	0.866	GPa
k_i	6.111	GPa
μ_i	4.583	GPa

inclusion. More precisely, the viscous behavior of masonry originated by that of the mortar matrix vanishes when the volume fraction of mortar tends to zero.

4.2. Comparison with the inverse LC method

The relaxation function in time space can be obtained by the inverse LC transformation of the effective stiffness tensor in LC space obtained by Eqs. (21) and (40)–(47). The effective shear component in the directions 1 and 2 that can be written as:

$$C^*_{hom,1212} = \mu_0^* + \frac{f}{\frac{1}{\mu_1-\mu_0^*} + \frac{1}{\mu_0^*}\left[S_1 + S_2 - 4\frac{\lambda_0^*+\mu_0^*}{\lambda_0^*+2\mu_0^*}S_9\right]} \quad (67)$$

with the coefficients μ_0^*, λ_0^* and k_0^* being computed from Eq. (10)

$$\mu_0^* = \left(\frac{1}{\mu_M} + \frac{1}{p\mu_v}\right)^{-1} + \mu_\infty; \; \lambda_0^* = k_0^* - \frac{2}{3}\mu_0^* \quad (68)$$

$$k_0^* = \left(\frac{1}{k_M} + \frac{1}{pk_v}\right)^{-1} + k_\infty \quad (69)$$

Mathematical platform such as Maple or Matlab can be employed to realize the inverse LC transformation but the analytical results obtained is extremely cumbersome and cannot be presented in this paper. Consider for example inclusions of dimensions $200 \times 50 \times 100\,(\mathrm{mm}^3)$ and joint thickness of 5 (mm) that correspond to a volume fraction $f = 0.845$. The correspondent geometric factors are: $S_1 = 0.019$, $S_2 = 0.092$, $S_9 = 0.00024$. Using also the viscoelastic parameters given in Table 1, we obtain the shear relaxation modulus in time space that is presented by the points on Fig. 6.

Now we return to the approximated method, we recall that the stress and strain relationship can be expressed by the simple and elegant differential Eq. (66) in time space. The relaxation modulus can be obtained using such equation without using the inverse LC transform. To do so, we consider a simple example where the constant macroscopic strain has the form $\boldsymbol{E} = E_0\underline{e_1} \otimes \underline{e_2}$, Eq. (66) becomes:

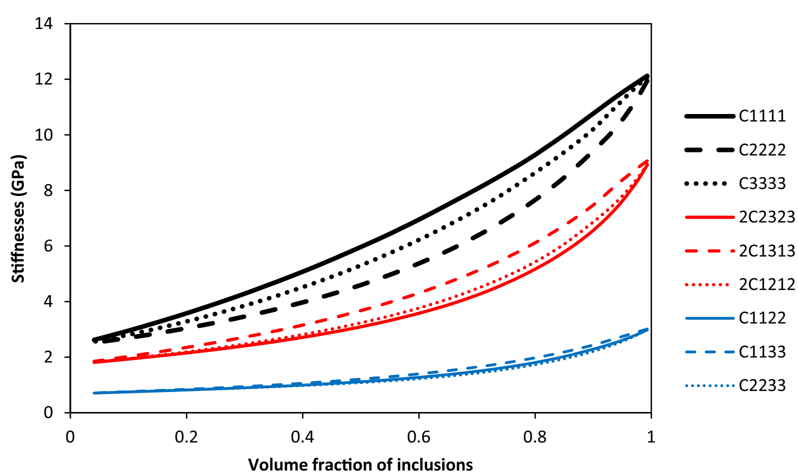

Fig. 3. Components of the long-term stiffness tensor as functions of the volume fraction of the inclusions.

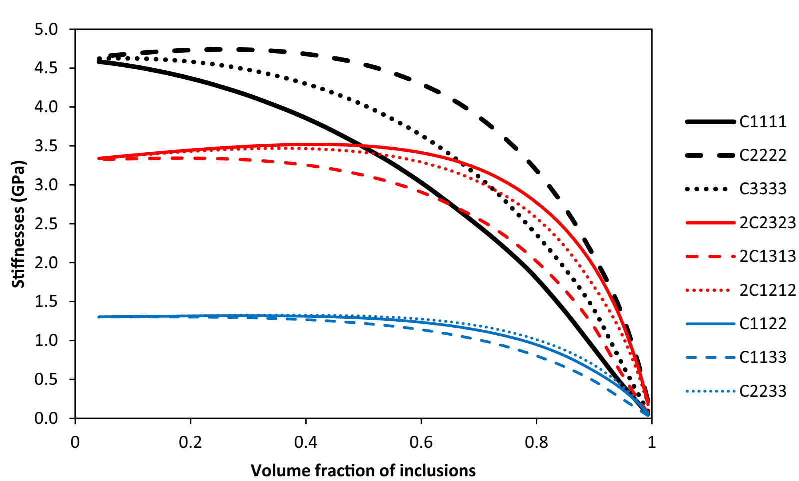

Fig. 4. Components of the stiffness tensor $\mathbb{C}_{Mhom}$ as functions of the volume fraction of the inclusions.

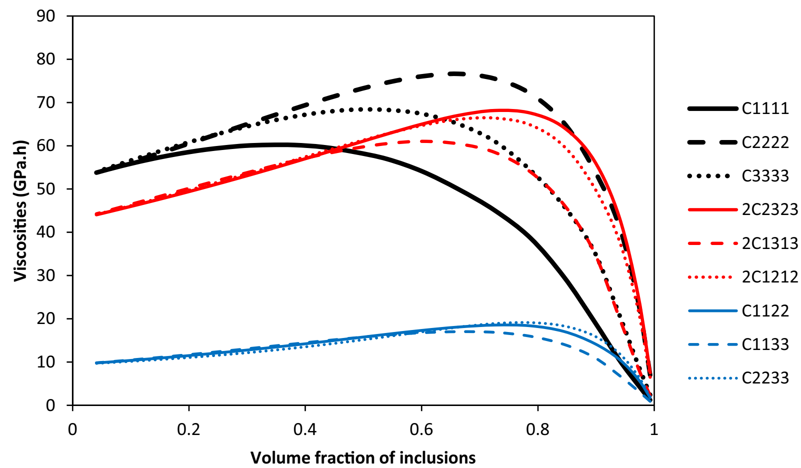

Fig. 5. Components of the viscous tensor $\mathbb{C}_{vhom}$ as functions of the volume fraction of the inclusions.

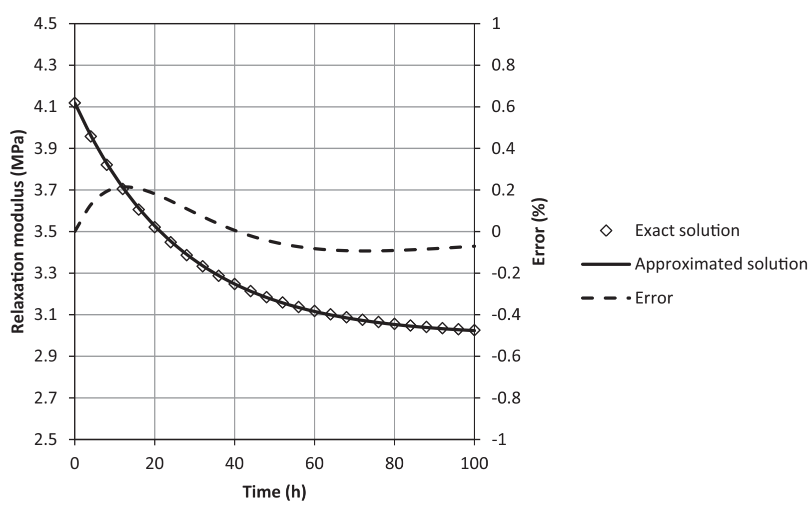

Fig. 6. Comparison of the presented method and the direct inverse LC method.

$$\Sigma_{12} + \frac{C_{vhom,1212}}{C_{Mhom,1212}}\dot{\Sigma}_{12} = 2C_{\infty hom,1212}E_0 \qquad (70)$$

The solution of Eq. (70) that satisfies the initial condition is the following

$$\Sigma_{12} = 2C_{\infty hom,1212}E_0 + 2C_{Mhom,1212}E_0 exp\left(-\frac{C_{Mhom,1212}}{C_{vhom,1212}}t\right) \qquad (71)$$

Then the shear relaxation modulus admits the form

$$R_{hom,1212} = \frac{\Sigma_{12}}{E_0} = C_{\infty hom,1212} + C_{Mhom,1212}exp\left(-\frac{t}{\tau_{hom,1212}}\right) \qquad (72)$$

where the relaxation time term $\tau_{hom,1212}$ is calculated with the expression

$$\tau_{hom,1212} = \frac{C_{vhom,1212}}{C_{Mhom,1212}} \qquad (73)$$

The latter corresponds to the effective shear characteristic time in directions 1 and 2. Fig. 6 shows a perfect validation of the proposed approach against the classical inverse LC method. Error between two methods is less than 0.3 (%).

It is also important to remark that, as the approximated method provides effective rheological viscoelastic properties, it can be easily implemented in a multi-scale homogenization scheme (as done by Nguyen et al. [23]), the self-consistent scheme or DEM model. Such techniques required n-steps homogenization procedure that can not be solved by the direct inverse LC method.

4.3. Impact of inclusion shape

To analyze the sensitivity of the effective viscoelastic properties of the mixture to the inclusion shape, we vary the first and second dimension of inclusions and fix its volume and third dimension, i.e. $b_1b_2b_3 = constant$ and $b_3 = constant$. Three brick types are considered namely $100 \times 100 \times 100\,(\mathrm{cm}^3)$; $200 \times 50 \times 100\,(\mathrm{cm}^3)$; $400 \times 25 \times 100\,(\mathrm{cm}^3)$. Figs. 7 and 8 show a strong impact of the inclusion shape on the overall viscoelastic properties of the mixture, especially at middle range of volume fraction of inclusions. A lower value of viscosity and a higher value of long-term stiffness are obtained for a higher value of b_1. Such dependence can be explained by the assumption of elastic inclusions. More precisely, a high value of b_1 reduce the viscosity effect in direction 1 of the mortar matrix on the overall behavior of the masonry.

4.4. Comparison between cubic and spherical inclusions

Now we focus on the case of cubic inclusion, i.e. $b_1 = b_2 = b_3$, the number of independent parameters of each viscoelastic tensor

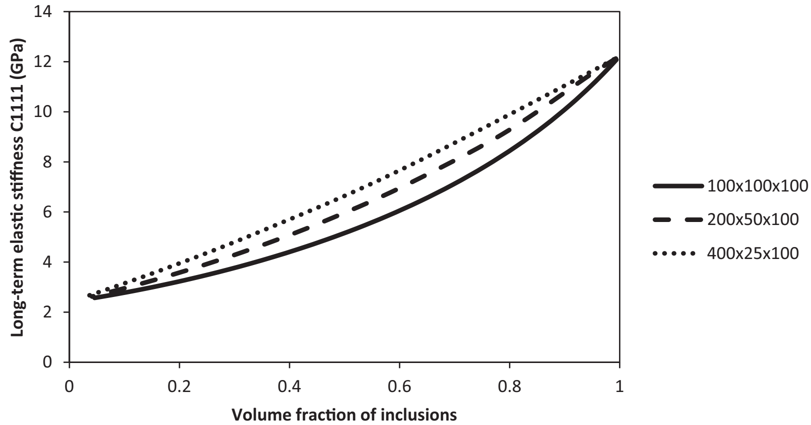

Fig. 7. Impact of the shape of inclusions on the long-term elastic stiffness.

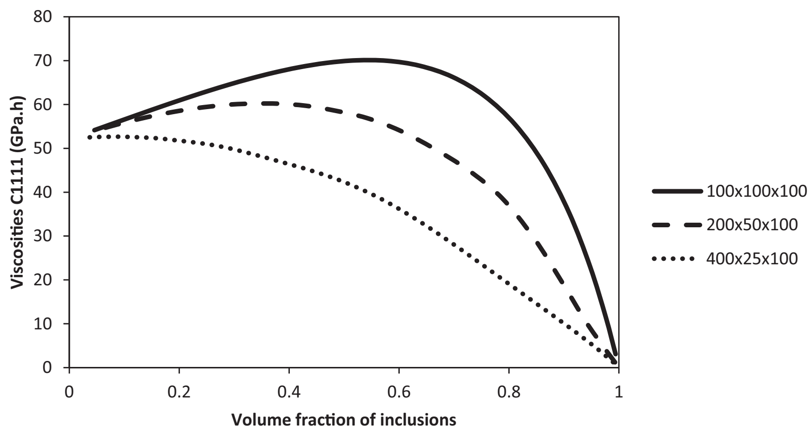

Fig. 8. Impact of the shape of inclusions on viscosity.

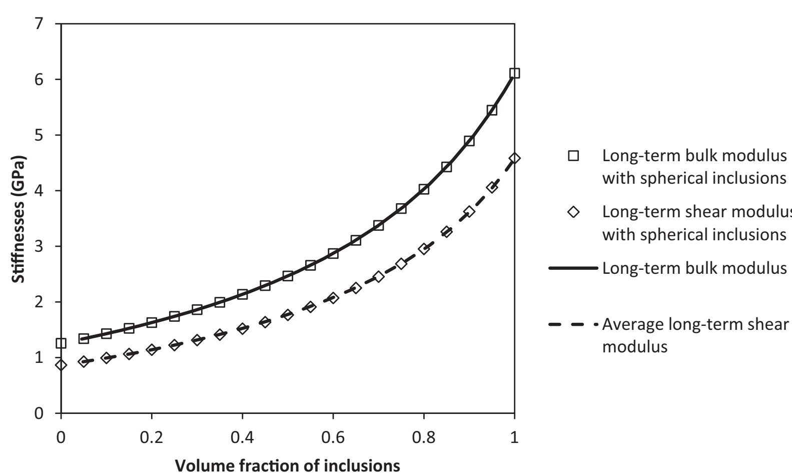

Fig. 9. Long-term bulk modulus and average shear modulus for the case of cubic inclusions and a comparison with that obtained for the case of spherical inclusion.

reduces to three: $C_{1111} = C_{2222} = C_{3333}$, $C_{1122} = C_{1133} = C_{2233}$, $C_{1212} = C_{1313} = C_{2323}$. The long-term bulk modulus is calculated by:

$$k_{\infty hom} = \frac{C_{1111,\infty hom} + 2C_{1122,\infty hom}}{3} \quad (74)$$

and the two independent shear moduli are given by:

$$\mu_{\infty hom} = C_{1212,\infty hom} \quad (75)$$

$$\mu'_{\infty hom} = \frac{C_{1111,\infty hom} - C_{1122,\infty hom}}{2} \quad (76)$$

Next, we define an average shear modulus as:

$$\mu^{average}_{\infty hom} = \frac{2\mu_{\infty hom} + \mu'_{\infty hom}}{3} \quad (77)$$

The dimensions of cubical inclusion are $100 \times 100 \times 100\,(\mathrm{cm}^3)$. Fig. 9 shows the long-term bulk modulus and average shear

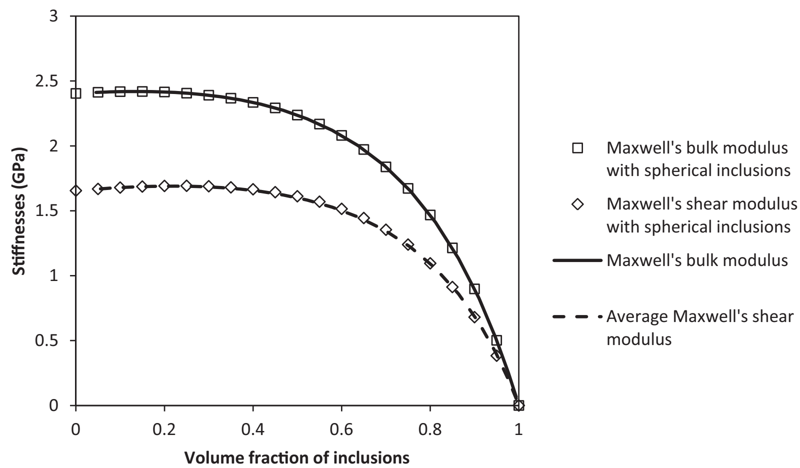

Fig. 10. Bulk modulus and average shear modulus of Maxwell's series for the case of cubic inclusions and a comparison with that obtained for the case of spherical inclusion.

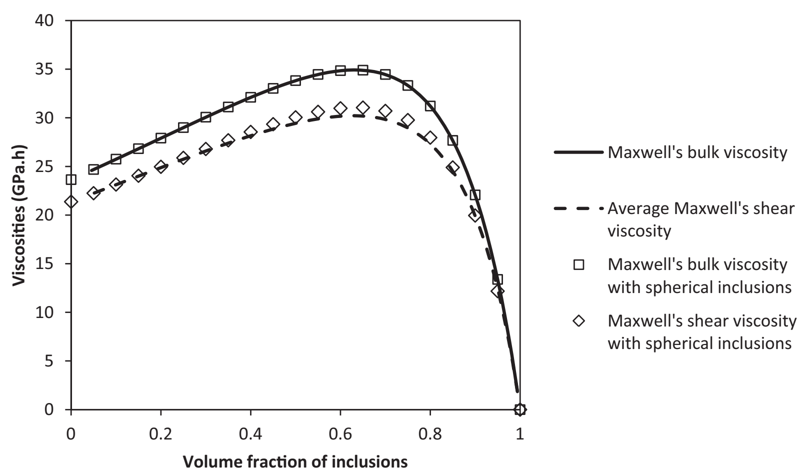

Fig. 11. Bulk viscosity and average shear viscosity of Maxwell's series for the case of cubic inclusions and a comparison with that obtained for the case of spherical inclusion.

modulus versus the volume fraction of the inclusions. These results are compared with the long-term bulk and shear moduli obtained for the case of spherical inclusions [23]. The long-term bulk modulus are identical for the cases of cubic and spherical inclusions while the average shear modulus of the case of cubic inclusions is almost identical to the shear modulus obtained for spherical inclusions.

Similarly, Figs. 10 and 11 present the comparison of the properties of the Maxwell's series between the cases of cubic inclusions and spherical inclusions. The effective elastic bulk and shear moduli and the bulk viscosity are also identical between the two cases of inclusion shape while the average shear viscosity obtained for the case of cubic inclusions is slightly smaller than the shear viscosity of medium containing spherical inclusions.

5. Conclusions

We derived analytical solutions for effective viscoelastic properties of periodic media containing cuboidal inclusions. The apparent effective stiffness tensor of a mixture of multi components is firstly derived in LC space considering the relationship between microscopic and macroscopic responses of the material. The geometric tensors and the apparent viscoelastic Hill tensors are obtained in the form of the Fourier series. The geometric tensors are functions of nine independent parameters that are in turn functions the dimensions of the inclusions and the unit periodic cell. The case of a mixture of a SLS viscoelastic matrix and elastic inclusions is then considered. The analytical solution in LC space is very well validated against numerical simulation using FEM on an equivalent elastic problem.

An application for masonry and a sensitivity analysis are given to illustrate the theoretical results. All the elastic stiffnesses and the viscosities of the Maxwell's series tend to zero when the volume fraction of brick tends to 1 due to the assumed elastic behavior of brick inclusions. Direct inverse LC transformation is also realized to validate the proposed approach. The sensitivity analysis shows also that the elastic behavior of the inclusions results also in a lower value of viscosity and a higher value of long-term stiffness in direction 1 for a higher value of b_1.

Finally, a comparison with the solutions obtained for the particular case of spherical inclusions is considered. For the case of cubic inclusions, the bulk elastic moduli and the bulk viscosity are identical to that obtained for the cases of spherical inclusions. Besides, the average shear moduli and shear viscosities of the case of cubic inclusions are almost identical or very close to that obtained for spherical inclusions.

References

[1] Caillerie D. Thin elastic and periodic plates. Math Methods Appl Sci 1984;6(1):159–91.
[2] Cecchi A, Sab K. A homogenized Reissner-Mindlin model for orthotropic periodic plates: Application to brickwork panels. Int J Solids Struct 2007;44(18):6055–79.

[3] Christensen RM. Viscoelastic properties of heterogeneous media. J Mech Phys Solids 1969;17(1):23–41.
[4] Dormieux L, Kondo D. Stress-based estimates and bounds of effective elastic properties: the case of cracked media with unilateral effects. Comput Mater Sci 2009;46(1):173–9.
[5] Dormieux L, Kondo D, Ulm FJ. Microporomechanics. Chichester: John Wiley & Sons; 2006.
[6] Hashin Z. Viscoelastic behavior of heterogeneous media. J Appl Mech Trans ASME 1965;32:630–6.
[7] Hashin Z. Complex moduli of viscoelastic composites – I. General theory and application to particulate composites. Int J Solids Struct 1970;6:539–52.
[8] Ignoul S, Schueremans L, Tack J, Swinnen L, Feytons S, Binda L, Van Balen K. Creep behavior of masonry structures–failure prediction based on a rheological model and laboratory tests. Struct Anal Historical Constr 2006;2:913–20.
[9] Kachanov M. Effective elastic properties of cracked solids: critical review of some basic concepts. Appl Mech Rev 1992;45(8):304–35.
[10] Kari S, Berger H, Rodriguez-Ramos R, Gabbert U. Computational evaluation of effective material properties of composites reinforced by randomly distributed spherical particles. Compos Struct 2007;77(2):223–31.
[11] Kari S, Berger H, Gabbert U, Guinovart-Dıaz R, Bravo-Castillero J, Rodrıguez-Ramos R. Evaluation of influence of interphase material parameters on effective material properties of three phase composites. Compos Sci Technol 2008;68(3):684–91.
[12] Lahellec N, Suquet P. Effective behavior of linear viscoelastic composites: a time-integration approach. Int J Solids Struct 2007;44(2):507–29.
[13] Le QV, Meftah F, He QC, Le Pape Y. Creep and relaxation functions of a heterogeneous viscoelastic porous medium using the Mori-Tanaka homogenization scheme and a discrete microscopic retardation spectrum. Mech Time-Depend Mater 2007;11(3–4):309–31.
[14] Lévesque M, Gilchrist MD, Bouleau N, Derrien K, Baptiste D. Numerical inversion of the Laplace-Carson transform applied to homogenization of randomly reinforced linear viscoelastic media. Comput Mech 2007;40(4):771–89.
[15] Nemat-Nasser S, Iwakuma T, Hejazi M. On composites with periodic structure. Mech Mater 1982;1:239–67.
[16] Nguyen TD, Duc ND. Evaluation of elastic properties and thermal expansion coefficient of composites reinforced by randomly distributed spherical particles with negative Poisson's ratio. Compos Struct 2016;153:569–77.
[17] Nguyen ST. Propagation of cracks and damage in non aging linear viscoelastic media. Paris-Est University; 2010 (Ph.D. thesis).
[18] Nguyen ST, Dormieux L, Le Pape Y, Sanahuja J. A Burger model for the effective behavior of a microcracked viscoelastic solid. Int J Damage Mech 2011;20(8):1116–29.
[19] Nguyen ST. Generalized Kelvin model for micro-cracked viscoelastic materials. Eng Fract Mech 2014;127:226–34.
[20] Nguyen ST, Dormieux L. Viscoelastic properties of transversely isotropic micro-cracked materials. Int J Damage Mech 2015. 1056789515575798.
[21] Nguyen ST, Vu MH, Vu MN, Nguyen TN. Generalized Maxwell model for micro-cracked viscoelastic materials. Int J Damage Mech 2015. 1056789515608231.
[22] Nguyen ST, Thai MQ, Vu MN, To QD. A homogenization approach for effective viscoelastic properties of porous media. Mech Mater 2016;100:175–85.
[23] Nguyen TN, Nguyen ST, Vu MH, Vu MN. Effective viscoelastic properties of micro-cracked heterogeneous materials. Int J Damage Mech 2015. 1056789515605557.
[24] Schapery RA. Stress analysis of viscoelastic composite materials. J Compos Mater 1967;1(3):228–67.
[25] Shufrin I, Pasternak E, Dyskin AV. Hybrid materials with negative Poisson's ratio inclusions. Int J Eng Sci 2015;89:100–20.
[26] To QD, Bonnet G, Hoang DH. Explicit effective elasticity tensors of two-phase periodic composites with spherical or ellipsoidal inclusions. Int J Solids Struct 2016;94–95:100–11.
[27] Wang YM, Weng GJ. The influence of inclusion shape on the overall viscoelastic behavior of composites. J Appl Mech 1992;59(3):510–8.